Linking Geostatistics with Basin and Petroleum System Modeling: Assessment of Spatial Uncertainties and Comparison with Traditional Uncertainty Studies

Bin Jia[1], Tapan Mukerji[2] and Allegra Hosford Scheirer[3]

Abstract Basin and Petroleum System Modeling spans a large spatial and temporal interval. Many of the input parameters are highly uncertain. Although probabilistic approaches based on Monte Carlo simulations have been used to address this uncertainty, the impact of spatial uncertainty on basin modeling remains unexplored. Lithologic facies is one of the key modeling inputs because rock properties such as porosity and thermal conductivity are wrapped into facies definition. Many techniques had been developed for facies modeling in reservoir characterization. These methods can be applied directly to basin modeling. In particular, multi-point geostatistical method has proved effective in facies modeling given sound training images. Another important spatial parameter is the geologic structure. Present day geologic structure is the initial point for reconstructing a sedimentary basin's depositional history. In this work we first show the uncertainty analysis in basin modeling in a traditional manner. Then the impact of geologic facies distribution and structural uncertainty from seismic time-to-depth conversion are studied. It is concluded that facies distribution has significant impact on the volume of oil accumulated. Further, different geological interpretations yield different results. Structural uncertainty from time-to-depth conversion has less impact in this case because the target area is fairly homogeneous.

Bin Jia[1] Stanford University, 367 Panama St #65, Stanford, CA, 94305, USA; currently at Aera Energy, 10000 Ming Avenue, Bakersfield, CA 93311, email: BJia@aeraenergy.com

Tapan Mukerji [2] Stanford University, 367 Panama St #65, Stanford, CA, 94305, USA email: mukerji@stanford.edu

Allegra Hosford Scheirer[3] Stanford University, 450 Serra Mall, MC2115, Stanford, CA, 94305, USA email: allegras@stanford.edu

Ninth International Geostatistics Congress, Oslo, Norway June 11 – 15, 2012

1. Introduction

Basin and Petroleum System Modeling (BPSM) is a key technology in hydrocarbon exploration that reconstructs deposition and erosion history and forward simulates thermal history and the associated generation, migration and accumulation of petroleum [8].

BPSM involves solving coupled nonlinear partial differential equations with moving boundaries. The equations govern deformation and fluid flow in porous media, coupled with chemical reactions and energy transportation. The coupled system has to be solved numerically on discretized time and spatial grids with the integration of geological, geophysical, and geochemical input. PetroMod uses the finite element method to solve these equations. The workflow and key input parameters are summarized in Figure 1 [8].

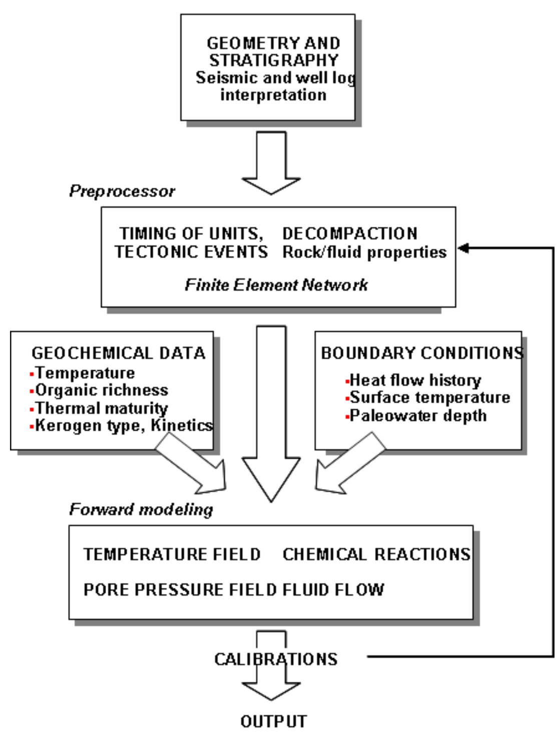

Figure 1: Basin and Petroleum System Modeling Workflow [8]

The modeling process can cover large spatial and temporal intervals. Many of the input parameters are highly uncertain and yield very different simulation results. Thus, understanding the impact of input parameters is critical for exploratory decision-making.

The interest in uncertainty analysis in BPSM increases as computer power makes it possible to assess multiple models in a reasonable time. While much work has been done on uncertainty analysis (e.g. [4, 12 and 13]), the focus is mainly on traditional Monte Carlo techniques, which randomly draw values from statistical distributions of the input parameter and compare the difference in the result for each drawn input parameter. This gives an estimate of parameter uncertainty but important spatial correlations are not taken into account. The outputs from these parameter Monte Carlo simulations cannot be used to assess the joint spatial uncertainty of the results. In earth sciences, one seldom has sufficient data to accurately reveal the entire underlying subsurface conditions. Typically in basin modeling one has to estimate the input parameters for the entire area with only a few data points. Spatial modeling techniques have to be used to make the best geological interpretation and understand the associated uncertainties.

Geologic facies is a key input for BPSM process because many important geophysical and petrophysical properties of the rocks are wrapped into the facies definition. Multi-point geostatistical (MPS) algorithm is the state-of-the-art method that generates multiple geological models that honor the geological interpretation and the well data at the same time. It is more suitable for facies modeling than traditional variogram-based methods. We will examine the impact of facies distribution by generating multiple facies map realizations using MPS method.

The present-day geologic structure model is the starting point for compaction analysis. Structure models are usually built based on picking and interpretation of seismic data with constraints at wells. Well data is considered exact, while each step of the seismic processing chain (acquisition, preprocessing, stacking, migration, interpretation, and time-to-depth conversion) has inherent uncertainty that must be evaluated and integrated into the final result. It is also pointed out that the time-to-depth conversion uncertainty often represents 50% or more of the total uncertainty in a model [11]. In this paper we study the impact of uncertainty in geologic structure using Bayesian kriging for seismic time-to-depth conversion. COHIBA software is used to generate multiple realizations of the structure model.

The rest of this paper is organized as the follows. Section 2 presents the traditional uncertainty analysis on parameters including TOC (Total Organic Carbon), HI (Hydrogen Index) and heat flow using PetroMod risking functionality. Section 3 studies the impact of facies uncertainty and section 4 studies structure uncertainty from seismic time-to-depth conversion. The results are compared with the traditional uncertainty assessment. Finally, a sampling method is proposed to reduce the number of models that are required in the ensemble-based workflow to evaluate total model uncertainty. The discussion ends with conclusions and future work.

2. Traditional uncertainty analysis

In this section we show the results of a traditional parameter uncertainty analysis on important parameters including TOC, HI and heat flow using a Monte-Carlo approach. PetroMod has built-in functionality for such kind of uncertainty analysis.

The generation and maturation of hydrocarbon components, molecular biomarkers, and coal macerals can be quantified by chemical kinetics, TOC and HI [5]. TOC is the ratio of the mass of all carbon atoms in the organic particles to the total mass of the rock matrix. HI is the ratio of the generative mass of hydrocarbon to the mass of organic carbon. HI multiplied with TOC and the rock mass is equal to the total generative mass of hydrocarbons in the rock [5].

Another important parameter usually risked is the heat flow at the base of the sediment, called basal heat flow. Magnitude, orientation, and distribution of the heat inflow at the base of the sediments are determined by mechanical and thermal processes of the crust and mantle [1].

2.1. Input model

A 3D synthetic layer cake model is used for our analysis (Figure 2). The model consists of five layers, and from bottom to top are: Underburden layer, Organic lean shale layer, Source rock layer, Reservoir rock layer and Overburden layer; these terms are defined in Magoon and Dow [6]. The model has 120 grid cells in the x direction and 30 in the y direction. Each grid cell represents a region of 1 km x 1 km area. The total region covers an area of 120 km x 30 km. The total depth is more than 4500 meters.

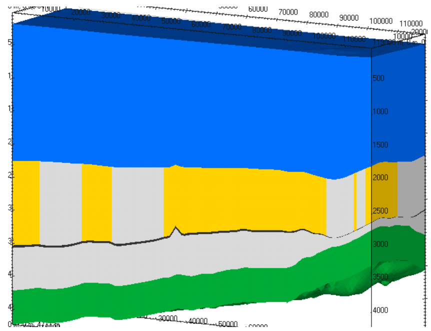

Figure 2: 3D display of the layer cake model

Figure 3 shows the same model in 2D sections. On the left is the vertical cross-section of the model; the thin dark layer in the middle is the organic-rich hydrocarbon source rock. The top right figure shows the lithologic facies of the reservoir rock layer in plan view. It consists two facies: sandstone (yellow) and organic lean shale (dark blue). The bottom right is the depth of the reservoir rock in plan view. The reservoir top is deeper on the left side and becomes shallower towards the right side.

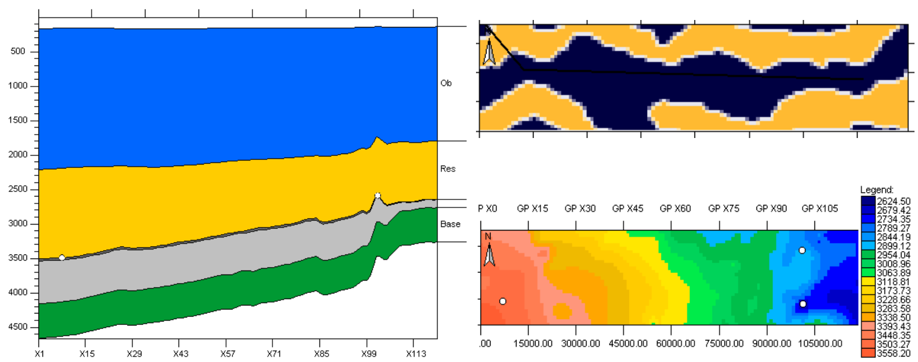

Figure 3: 2D view of the input model. Left: Vertical section; Top right: facies map of reservoir layer in plan view; Bottom right: depth map of the reservoir layer in plan view.

The deposition setting is summarized in Figure 4. Each layer is deposited over a 10 million year timespan except for the source rock layer, which is formed in 1 Ma. The reservoir layer has a channel fluvial depositional setting and is made of two types of facies. Erosion is not considered in this scenario.

Name	Color	Deposition Age from [Ma]	Deposition Age to [Ma]	Erosion Age from [Ma]	Erosion Age to [Ma]	Max. Time Step Duration [Ma]	Facies 1	Facies 2
Ob		10.00	0.00	0.00	0.00	10.00	Fac_OB	---
Res		20.00	10.00	0.00	0.00	10.00	Fac_Res	Fac_Seal
Src_up		21.00	20.00	0.00	0.00	10.00	Fac_Src	---
Src_lean		30.00	21.00	0.00	0.00	10.00	Fac_Seal	---
Base		40.00	30.00	0.00	0.00	10.00	Fac_UB	---

Figure 4: Age assignment of each layer

The lithologic facies definition is summarized in Figure 5. The source rock layer is assigned a lithology of “Shale (typical)”, which has 5% TOC and an HI of 500 mg hydrocarbons per gram of TOC. The kinetics of Pepper&Corvi (1995)_TII(B) is used, indicating an oil prone source rock. The reservoir layer contains both typical sandstone and organic lean shale. The sandstone acts as the trap for generated hydrocarbons and the shale acts as a barrier for fluid flow.

Name	Color	Lithology Value	TOC Value [%]	Kinetics	HI Value [mgHC/gTOC]
Fac_OB		Siltstone (organic lean)	0.00	none	0.00
Fac_Res		Sandstone (typical)	0.00	none	0.00
Fac_Src		Shale (typical)	5.00	Pepper&Corvi(1995)_TII(B)	500.00
Fac_UB		Siltstone (organic lean)	0.00	none	0.00
Fac_Seal		Shale (organic lean, typical)	0.00	none	0.00

Figure 5: Facies definition of major lithologies.

The boundary conditions required by PetroMod are shown in Figure 6. We accept default values for each. These are: heat flow of 60 mW/m², paleowater depth of 0 m, and surface temperature of 20° C.

Time (Ma)	Value (m)	Time (Ma)	Value (C)	Time (Ma)	Value (mW/m^2)
Water Depth	Water Depth	SWI	SWI	Heat Flow	Heat Flow
Default1	Default1	Default	Default	Default	Default
200.00	0.00	200.00	20.00	200.00	60.00
0.00	0.00	0.00	20.00	0.00	60.00

Figure 6: Boundary conditions

The initial simulation result is shown below in Figure 7. The total oil accumulation in the reservoir rock layer is about 1378 MMbbls. The oil was generated from the source rock layer and migrates up to the reservoir layer. The oil then continues to move toward the high elevation area. The organic lean shale in the reservoir layer acts as the flow barrier, allowing the accumulation of oil in simulated stratigraphic-type traps.

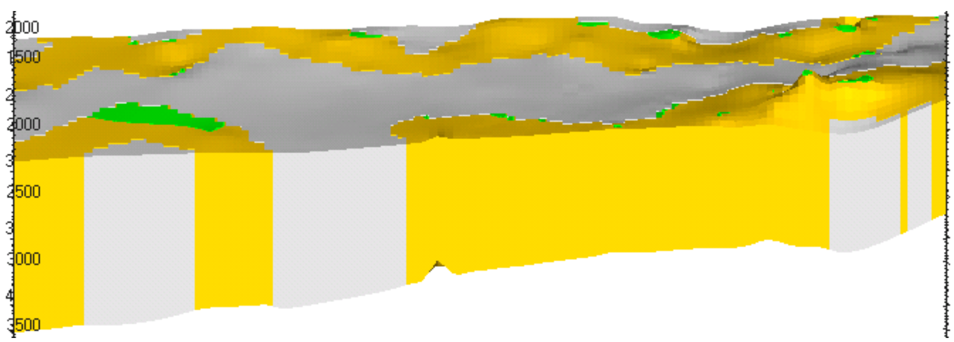

Figure 7: Simulation result for the base case with oil accumulation of 1378 MMbbls

2.2. TOC

We first performed the risking analysis on TOC values. An extensive range of TOC value from 1% to 10% is studied. We see the oil accumulation increases as the TOC value increases. The total accumulation varies from 500 to 2300 MMbbls. Typical values of TOC range from 3% to 7%, and correspondingly the oil accumulation varies from 1100 to 1700 MMbbls. Figure 8 shows the simulation results and also the estimated oil accumulation distributions.

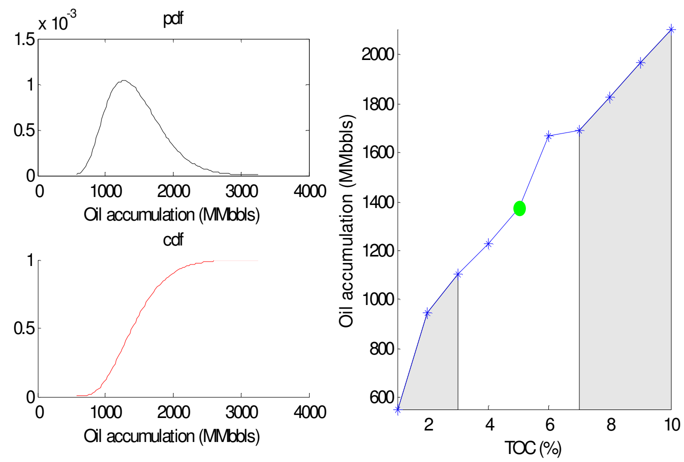

Figure 8: TOC risking results. The estimated distribution gives P10 of 973, P50 of 1395 and P90 of 1992 MMbbls.

2.3. HI

A similar study is performed for hydrogen index. For the typical HI value ranging from 300 to 700 mgHC/gTOC, the oil accumulation is between 1100 and 1700 MMbbls. We see the result is similar to the result of TOC risking.

2.4. Heat flow

Heat flow is another uncertain parameter for risk analysis is commonly performed in basin modeling. We tested a range of heat flow values around the default value of 60 mW/m². At very low heat flow values there is no oil accumulation due to the absence of hydrocarbon generation. As the value increases to above 40 mW/m² the oil accumulation increases dramatically and reaches a peak at a heat flow of 50 mW/m². Then the oil accumulation starts to decrease because of secondary cracking—oil is cracked into gas. Figure 10 shows that gas starts to accumulate when heat flow is above 60 mW/m².

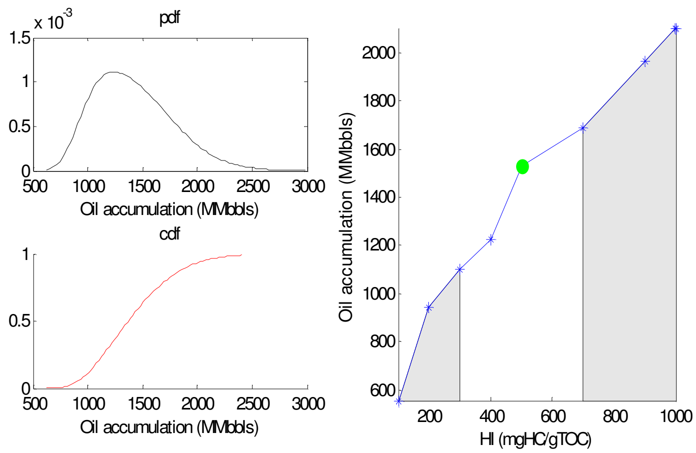

Figure 9: HI risking result. The estimated distribution gives P10 of 981, P50 of 1368 and P90 of 1905 MMbbls

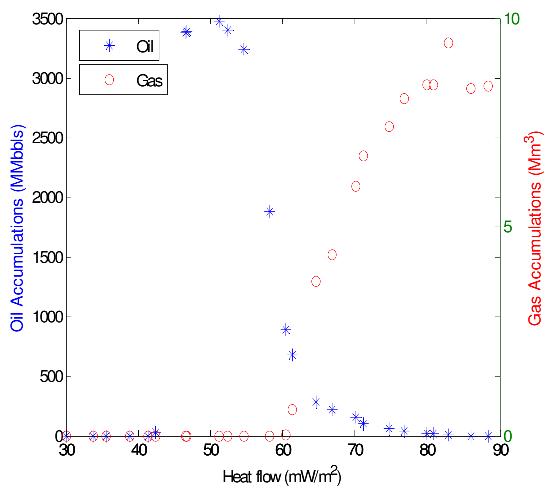

Figure 10: Heat flow results. Oil accumulation starts at 43 mW/m^2 and gas generation activates at heat flow above 60 mw/m^2.

3. Facies uncertainty

We now turn to the spatial uncertainty associated with spatially heterogeneous lithologic facies distribution. Assume that the reservoir rock consists of mainly two facies, sand and shale, in a channel depositional environment. From estimated channel width, wavelength, and amplitude, a training image is created representing the best conceptual geological understanding of the spatial distribution. In addition a few well logs are available as hard constraints. With all these available data, one can build multiple facies maps for the reservoir rock layer using multiple-point geostatistical algorithms. We used SNESIM [10] to generate facies realizations from the training image, conditioned to the well data. Figure 11 shows 4 possible realizations out of the 50 realizations from SNESIM. All these facies maps have the same shale to sand ratio of 50%:50%.

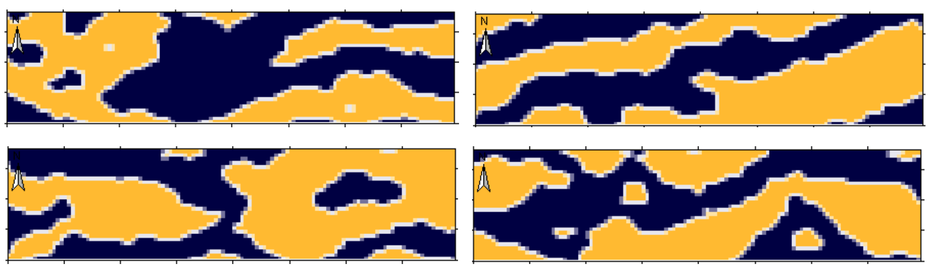

Figure 11: Four facies map selected from the 50 realizations. Yellow color represents sandstone and dark blue is organic lean shale

All these models were input into PetroMod for simulation, yielding 50 different scenarios for volume and distribution of oil; these 50 models used the same parameters and boundary conditions as in the initial model. For difference facies distribution, we get P10 of 558, P50 of 965 and P90 of 1848 MMbbls (Figure 12).

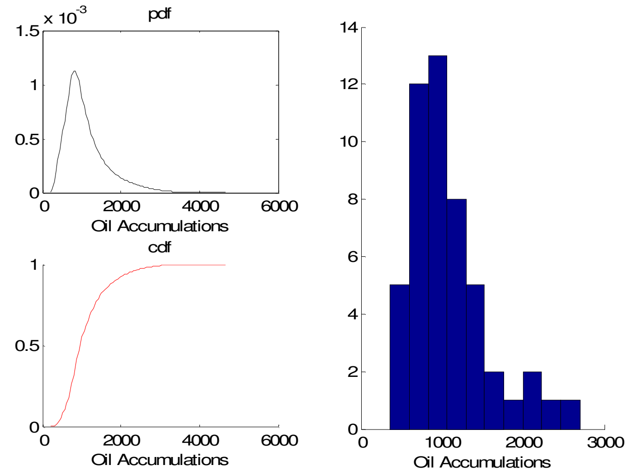

Figure 12: Oil accumulations for 50 realizations

To compare the impact of uncertainty in spatial distribution of lithologic facies to other modeling inputs, the mean and standard deviation are calculated and shown in Figure 13. We can see that the facies distribution has similar impact as TOC and HI on volume of accumulated oil. Thus it should also be considered as an important parameter for risking analysis.

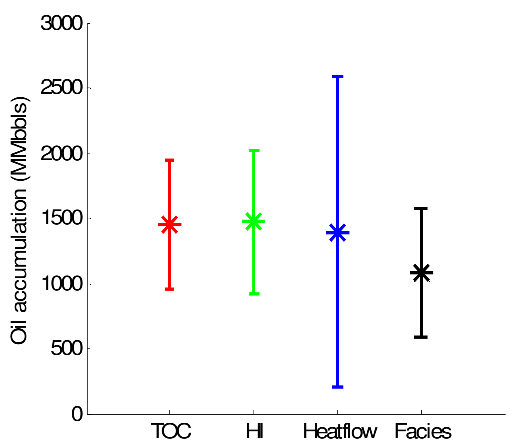

Figure 13: Mean and standard deviation for different parameters

Another important factor is that besides the volume of oil accumulation, the spatial pattern of oil accumulation is also different. Four simulation results are shown below Figure 14 in which the green polygons illustrate discrete oil accumulations. We can see that for different lithologic facies distributions, the geometric distributions of oil accumulations differ.

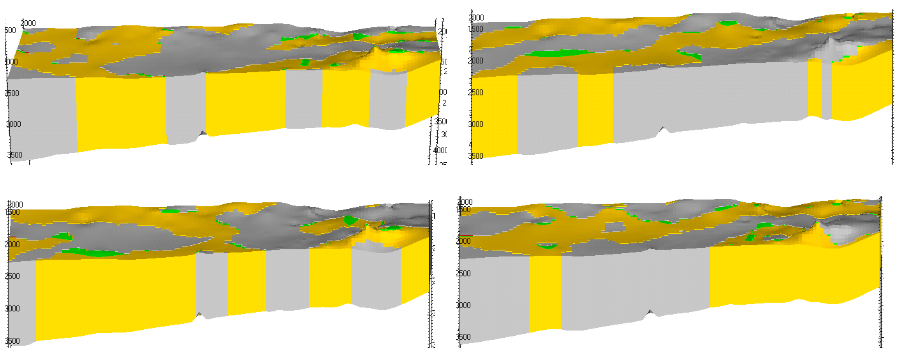

Figure 14: Different oil accumulation patterns

3.1. Homogeneous reservoir layer

In basin and petroleum system modeling, it is common that modelers will select a homogeneous lithology for an entire model layer even when the layer was deposited over great geologic distances and/or timespans. We studied this scenario by assigning a typical sandstone lithology for the entire reservoir rock layer in our 3D model. The result is shown in Figure 15. The oil accumulation volume is surprisingly low, with only 310 MMbbls.

Figure 15: Oil accumulation is only 310 MMbbls for a homogeneous reservoir layer

3.2. Different training image

We selected another geologic scenario to condition the training image for the reservoir rock layer in the basin model. Figure 16 shows several realizations of a more heterogeneous scenario, that of a delta environment.

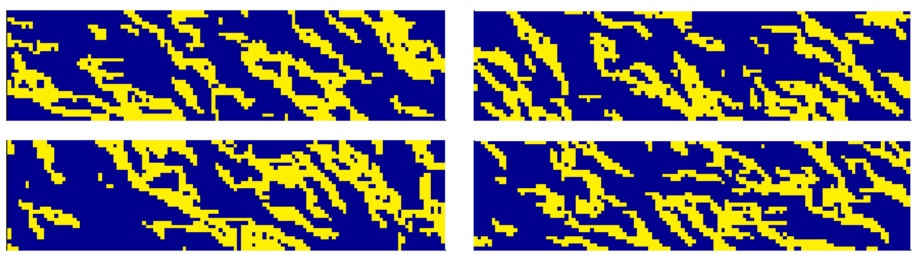

Figure 16: Facies distribution maps using a more heterogeneous training image

Again 50 simulations were performed with all other settings exactly the same as before. The result is compared against the results above. We can see in Figure 17 that the oil accumulation distribution is quite different from the previous models. There is much more oil accumulated with the mean value of 3082 MMbbls. The variance is also higher with a standard deviation of 1006.

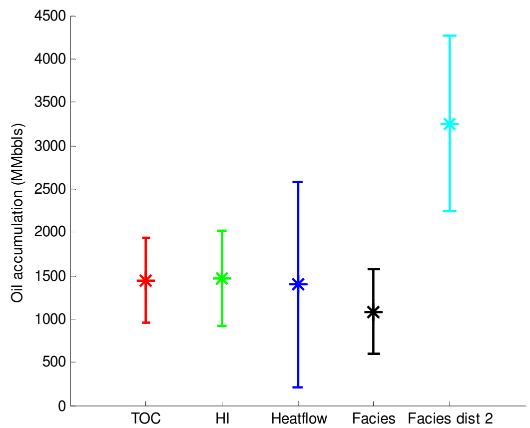

Figure 17: Results for a different training image is quite different from the example above. Both mean and variance are higher for the more heterogeneous scenario

4. Structural uncertainty

Structural models for a basin are usually constructed based on depths determined from two-way seismic travels times supplemented by depths from well logs. The well data are accurate to within a few meters, but are usually available at scattered locations. In contrast, seismic travel times are usually available on a spatially extensive grid, which allows an almost continuous but inexact description of the lateral depth trends. Many geostatistical methods have been developed to combine the exact well measurements with seismic travel time data to make the best prediction of the structure model and quantify the associated uncertainties. Abrahamsen [3] compared different methods and concluded that Bayesian kriging is one of the more suitable approaches for depth prediction because all data are included and all intercorrelations between surfaces and interval velocity fields are considered.

Traditionally the time-to-depth conversion is performed for each layer independently. Abrahamsen [2] proposed an approach to integrate all surfaces and the estimated velocity field in one consistent model using Bayesian kriging, as described in Omre and Halvorsen [7]. The approach is briefly summarized here.

The travel time $t_l(x)$ is considered as an average of an area, so the ‘true’ travel time to the reflector l is modeled with a residual as

$$T_l(x) = t_l(x) + R_l^t(x)\,. \tag{1}$$

The interval velocity is modeled with a lateral trend and residual as

$$V_l(x) = \sum_{p=1}^{P_l} A_l^p g_l^p(x) + R_l^v(x)\,, \tag{2}$$

where A_l^p are the prior coefficient parameters, g_l^p are the known regression functions which are typically interval velocities from stacking velocities or functions of interpreted travel times. The model can be formulated as

$$Z(x) = \sum_{l=1}^{L}\sum_{p=1}^{P_l} A_l^p g_l^p(x)\Delta t_l(x) + \sum_{l=1}^{L} R_l^v(x)\Delta t_l(x) + R_L^z(x)\,, \tag{3}$$

where Z(x) is the depth to surfaces. The Bayesian kriging predictor and the corresponding variance are

$$\begin{aligned} Z^*(x) &= f(x)\cdot\mu_0 + \mathrm{k}_z(x)K_z^{-1}(Z - F\mu_0) \\ \sigma^*(x) &= k_z(x) - \mathrm{k}_z(x)K_z^{-1}\mathrm{k}_z^T(x)\,, \end{aligned} \tag{4}$$

Where

$$f(x) = \sum_{l=1}^{L} g_l(x)\Delta t_l(x)\,. \tag{5}$$

μ_0 is the prior mean of coefficient parameters A, $k_z(x)$ is the prior variance of Z(x), $\mathrm{k}_z(x)$ is the prior covariance between Z(x) and the data vector Z, and K_z is the covariance matrix.

The key advantage of Bayesian kriging is that unlike kriging-with-trend, it is stable for any number of coefficients and data, including cases without well observations [3]. This is important for basin structural modeling because it is usually done at an early stage of exploration when very few well data are available.

4.1. Depth maps

The geologic structure of a hydrocarbon reservoir rock is an important factor for oil accumulations. We are interested to assess the impact of oil accumulation due to uncertainty in reservoir layer interpretation. A synthetic time map is generated for the reservoir layer shown below (Figure 18).

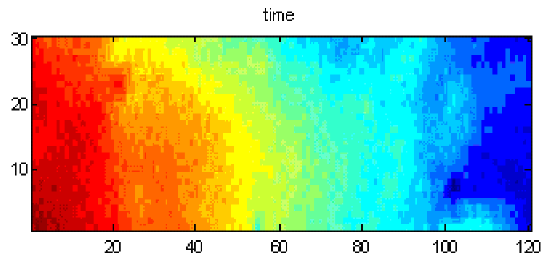

Figure 18: Synthetic time map

Multiple depth maps are then generated from the time map using the COHIBA software that performs Bayesian kriging. Two well points are available as exact data; these are located at coordinates (102, 8) and (11, 21). Figure 19 shows the predicted depth maps at the top part and the corresponding error at the bottom part. The depth prediction is exact at the well location and the error is small near the wellbore region. However, it is clear that with only two well constraints, the predicted depth throughout the rest of the region can be incorrect by more than 300 meters.

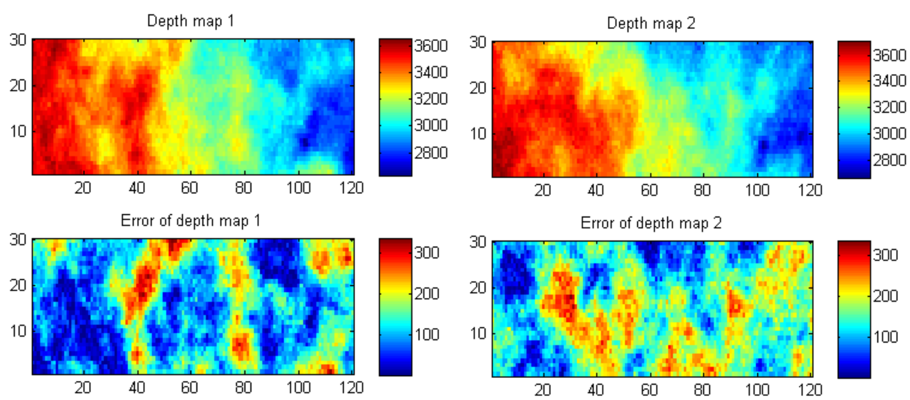

Figure 19: Multiple realizations of depth map and the corresponding errors

Ten realizations of the reservoir rock depth are generated and input into PetroMod for simulation. The result is shown in Figure 20. We see that there are differences in the volume of accumulated oil, but that the uncertainty is smaller compared to the previous examples. One reason could be that the depth variations are localized and the overall structure is still very similar.

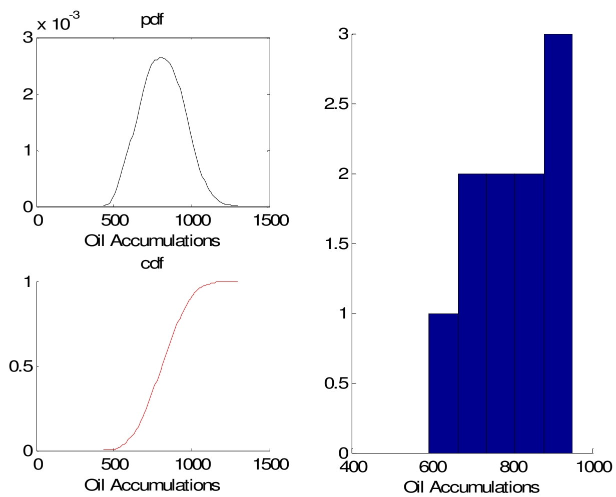

Figure 20: Oil accumulation for different depth realizations

5. Reducing the number of simulations

We have just shown that spatial uncertainty of lithologic facies distributions is an important factor in the overall uncertainty of a basin and petroleum system model. In the example above, 50 facies map realizations were studied. However, the generation and simulation of 50 models in BPSM is time consuming. For the spatially limited (120 x 30) models we have, this experiment required tens of hours to do the simulation for all the models. Because spatial uncertainty analysis in basin and petroleum system modeling is still in its infancy, modeling with ensembles of facies distributions is not yet an automated functionality in any BPSM package. This means that one has to do a significant amount of manual work. The question is can we reduce the amount of models that are required for simulation and still get a good approximation of the uncertainty profile? One approach is to use distance and kernel methods [9]. Using multi-dimensional scaling (MDS), with an appropriate distance metric, multiple models are mapped to a low-dimensional space. Kernel clustering method is then used in the low-dimensional space to select a subset of realizations that are representative for the uncertainty space. We used the Euclidean distance to do MDS using the 50 facies realizations. Figure 21 shows the plot of the 50 realizations in two dimensions, and the 7 clusters from kernel K-means clustering.

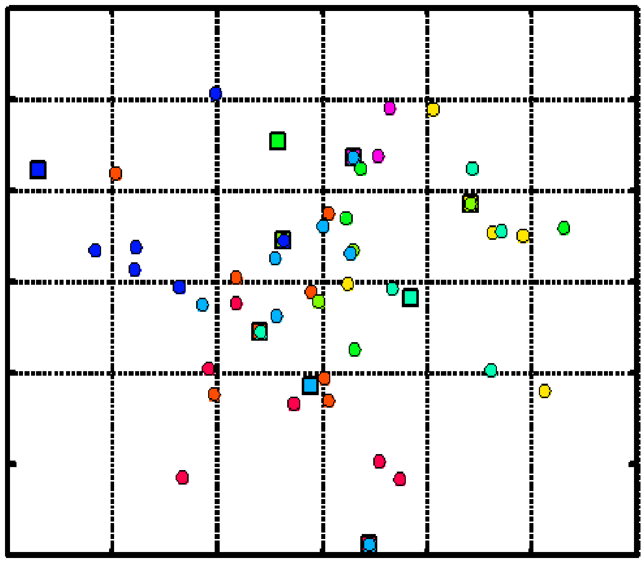

Figure 21: Facies maps displayed in metric space in clusters

Is the subset of 7 realizations a good representative of the uncertainty space from 50 realizations? Figure 22 shows the oil accumulation for the 7 selected models (blue dots) on top of all the 50 realizations (red stars). The accumulated oil volume through time is plotted for each model. We see that the 7 selected realizations span most of the original uncertainty space, though some extreme values are missed.

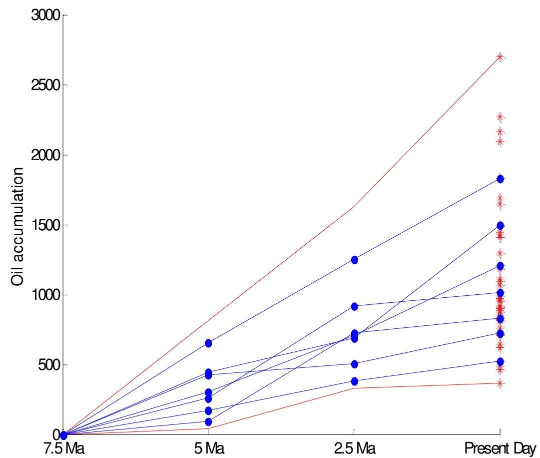

Figure 22: The 7 selected models (blue) span the most part of the prior distribution from 50 models (red)

Figure 23 compares the pdf and cdf of oil accumulation from the subset of selected realizations to the ones obtained from all 50 realizations. Again we see a good match showing that the 7 models can reasonably capture the distribution from the 50 models.

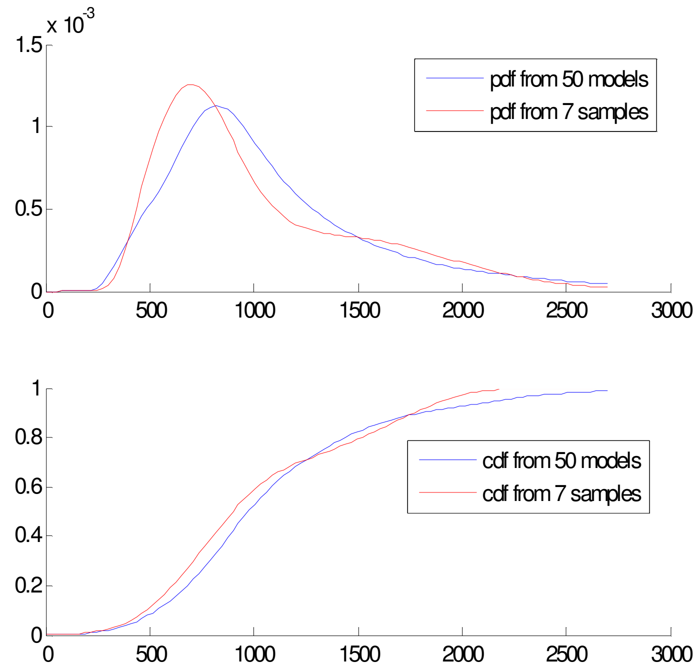

Figure 23: Comparison of 7 models from kernel K-mean clustering to the 50 prior models shows a good match for estimated pdf and cdf

6. Conclusions and future work

Uncertainty is an intrinsic complication in Basin and Petroleum System Modeling because of the large spatial and temporal scale of the problem. The traditional methodology is to do Monte Carlo simulations on the input parameters. This is done in this study as the benchmark. The spatial uncertainties including facies and structure are not studied before. We applied the geostatistical methods to generate multiple realizations of facies and structure map. The corresponding uncertainty in oil accumulation and oil distribution is assessed. We showed that facies distribution has a great impact on the simulation results and different geological interpretation could lead to very different results. In fact, variations in the volume of accumulated oil due to lithologic facies variations are equally if not more important than variations in TOC, HI, and basal heat flow. Thus it is important that the modeling process account for both varying lithologies within a reservoir rock and the spatial correlation among them. Structure uncertainty on the other hand does not have as great impact in this example as we expected. One reason is that we only considered the uncertainty in time-to-depth conversion assuming the seismic picks are perfect. One important future work is to investigate different time horizon interpretations.

7. Acknowledgement

The authors would like to thank Ken Peters, Les Magoon, and Oliver Schenk for their help. Special thanks to Petter Abrahamsen for providing the COHIBA software package. We would also like to thank Schlumberger for the PetroMod license, and the sponsors of the Stanford Basin and Petroleum System Modeling (BPSM) consortium and Stanford Center for Reservoir Forecasting (SCRF) for their support.

Bibliography

[1] Allen P. A. and Allen J. R., Basin Analysis. Blackwell Publishing, second edition, 2005.

[2] Abrahamsen, P., 1992. Bayesian Kriging for seismic depth conversion of a multi-layer reservoir, Fourth International Geostatistical Congress. Troia, Portugal September 13-18.

[3] Abrahamsen, P., 1996, Geostatistics for Seismic Depth Conversion. Report, NR-note SAND/06/1996, 9 pages.

[4] Corradi A., D. Ponti, P. Ruffo, and G. Spadini, 2003, A methodology for prospect evaluation by probabilistic basin modeling, in S. Düppenbecker and R. Marzi, eds., Multidimensional basin modeling, AAPG/Datapages Discovery Series No. 7, p. 283– 293.

[5] Hantschel, T., Kauerauf, A., 2009. *Fundamentals of Basin Modeling*. Springer-Verlag, Heidelberg, 425 pp.

[6] Magoon, L. B., and Dow, W. G., 1994, The Petroleum System: From Source to Trap, American Association of Petroleum Geologists Memoir 60, Tulsa, Oklahoma, 655 p.

[7] Omre, H., Halvorsen, K. B., 1989. The Bayesian bridge between simple and universal kriging. Math. Geol., 21(7):767-785.

[8] Peters, K. E., 2009, Getting Started in Basin and Petroleum System Modeling. American Association of Petroleum Geologists (AAPG) CD-ROM #16, AAPG Datapages.

[9] Scheidt C., Caers J., A new method for uncertainty quantification using distances and kernel methods. Application to a deepwater turbidite reservoir. SPE J, 14 (4): 680-692, SPEJ 118740-PA

[10] Strebelle, S., 2002, Conditional Simulation of Complex Geological Structures Using Multiple-Point Statistics: Mathematical Geology, v. 34, no. 1, p. 1-22.

[11] Thore, P., A. Shtuka, M. Lecour, T. Ait-Ettajer, and R. Cognot, 2002, Structural uncertainties: Determination, management, and applications: Geophysics, 67, 840–852.

[12] Wendebourg, J., 2003, Uncertainty of petroleum generation using methods of experimental design and response surface modeling: Application to the Gippsland Basin, Australia, in S. Düppenbecker and R. Marzi, eds., Multidimensional basin modeling, AAPG/Datapages Discovery Series No. 7, p. 295– 307.

[13] Zwach, C., and D. Carruthers, 1998, Honouring uncertainties in the modelling of migration volumes and trajectories (abs.): IFE Symposium on Advances in Understanding and Modelling Hydrocarbon Migration, Oslo, Norway, December 7–8, 1998.